Received: 19 December 2018 | Revised: 1 July 2019 | Accepted: 12 August 2019

DOI: 10.1002/ajmg.a.61342

ORIGINAL ARTICLE

AMERICAN JOURNAL OF medical genetics PART A WILEY

Duplication 2p16 is associated with perisylvian polymicrogyria

Dina Amrom[1,2,3] | Annapurna Poduri[4,5] | Jennifer S. Goldman[6] | Bernard Dan[3] | Nicolas Deconinck[3] | Bruno Pichon[7] | Javad Nadaf[8,9] | Frederick Andermann[2,10,11†] | Eva Andermann[1,2,8,10] | Christopher A. Walsh[5,12,13] | William B. Dobyns[14]

[1]Neurogenetics Unit, Montreal Neurological Institute and Hospital, Montreal, Quebec, Canada

[2]Department of Neurology & Neurosurgery, McGill University, Montreal, Quebec, Canada

[3]Department of Neurology, Hôpital Universitaire des Enfants Reine Fabiola (HUDERF), Université Libre de Bruxelles (ULB), Brussels, Belgium

[4]Division of Epilepsy & Clinical Neurophysiology, Children's Hospital, Boston, Massachusetts

[5]Department of Neurology, Children's Hospital, Boston, Massachusetts

[6]Ludmer Centre for Neuroinformatics and Mental Health and the Department of Biomedical Engineering, McGill Centre for Integrative Neuroscience, McGill University, Montreal, Quebec, Canada

[7]Department of Medical Genetics, Hôpital Erasme, Université Libre de Bruxelles (ULB), Brussels, Belgium

[8]Department of Human Genetics, McGill University, Montreal, Quebec, Canada

[9]Genome Quebec Innovation Center, McGill University, Montreal, Quebec, Canada

[10]Epilepsy Research Group, Montreal Neurological Institute and Hospital, Montreal, Quebec, Canada

[11]Department of Pediatrics, McGill University, Montreal, Quebec, Canada

[12]Division of Genetics and Manton Center for Orphan Disease Research, Children's Hospital, Boston, Massachusetts

[13]Howard Hughes Medical Institute, Harvard Medical School, Boston, Massachusetts

[14]Department of Pediatrics (Genetics) and Neurology, University of Washington, and Seattle Children's Research Institute, Seattle, Washington

Correspondence
Dina Amrom, Department of Neurology, Hôpital Universitaire des Enfants Reine Fabiola, 15, Avenue JJ Crocq, 1020 Brussels, Belgium.
Email: dina.amrom@ulb.ac.be, dina.amrom@huderf.be

William B Dobyns, Seattle Children's Research Institute, Center for Integrative Brain Research, 1900 Ninth Avenue, M/S JMB-10, Seattle WA 98101.
Email: wbd@uw.edu

Present address
Dina Amrom, Bernard Dan: Department of Neurology, Hôpital Universitaire des Enfants Reine Fabiola (HUDERF), Université Libre de Bruxelles (ULB), Brussels, Belgium.

Dina Amrom: Division of Neurology, Kannerklinik, Centre Hospitalier de Luxembourg, Grand-Duchy of Luxembourg.

Bernard Dan: Inkendaal Rehabilitation Hospital, Vlezenbeek, Belgium.

Abstract

Polymicrogyria (PMG) is a heterogeneous brain malformation that may result from prenatal vascular disruption or infection, or from numerous genetic causes that still remain difficult to identify. We identified three unrelated patients with polymicrogyria and duplications of chromosome 2p, defined the smallest region of overlap, and performed gene pathway analysis using Cytoscape. The smallest region of overlap in all three children involved 2p16.1-p16.3. All three children have bilateral perisylvian polymicrogyria (BPP), intrauterine and postnatal growth deficiency, similar dysmorphic features, and poor feeding. Two of the three children had documented intellectual disability. Gene pathway analysis suggested a number of developmentally relevant genes and gene clusters that were over-represented in the critical region. We narrowed a rare locus for polymicrogyria to a region of 2p16.1-p16.3 that contains 33–34 genes, 23 of which are expressed in cerebral cortex during human fetal development. Using pathway analysis, we showed that several of the duplicated genes contribute to neurodevelopmental pathways including morphogen, cytokine, hormonal and growth factor signaling, regulation of cell cycle progression, cell morphogenesis, axonal guidance, and neuronal migration. These findings strengthen the

[†]Died June 16, 2019.

Christopher A Walsh and William B Dobyns contributed equally to the manuscript.

 © 2019 Wiley Periodicals, Inc.

Funding information
National Institute of Neurological Disorders and Stroke (NINDS), Grant/Award Numbers: 1R01NS035129, 1R01NS058721, P01NS039404

evidence for a novel locus associated with polymicrogyria on 2p16.1-p16.3, and comprise the first step in defining the underlying genetic etiology.

KEYWORDS
chromosome 2, duplication 2p16.1-p16.3, growth retardation, intellectual disability, polymicrogyria

1 | BACKGROUND

Polymicrogyria (PMG) is a malformation of cortical development that is classified according to its lobar topography. It represents a clinically, radiologically, and etiologically heterogeneous group of conditions. Among genetic causes, single gene mutations have been associated with several specific patterns of PMG, although genetic testing is negative in a majority of patients (Barkovich, Guerrini, Kuzniecky, Jackson, & Dobyns, 2012; Jansen & Andermann, 2005; Stutterd & Leventer, 2014). Chromosomal copy number variants (CNVs) are another established cause of PMG, the most frequent being deletion 22q11.2 and deletion 1p36.3 (Dobyns et al., 2008; Jansen & Andermann, 2005; Robin et al., 2006), while rare CNVs have involved 1p31.3-p31.1, 1p34.1, 2p16.1-p23.1, 4q21.21-q22.1, 6q26-q27, 11p14.3-p14.2, and 21q21.3-q22.1 with variable clinical and radiological expression (Dobyns et al., 2008; Sajan et al., 2013).

Here we report three patients from three unrelated families presenting common phenotypic features characterized by developmental delay, similar dysmorphic facial features, intrauterine and postnatal growth deficiency, intellectual disability (ID), and bilateral perisylvian polymicrogyria (BPP), all of whom harbor overlapping duplications of chromosome 2p. Using single nucleotide polymorphism (SNP) microarrays, we narrowed the locus for BPP to 2p16.1-p16.3. A number of duplicated genes in this locus are expressed during development of the cerebral cortex and are strong candidates to contribute to abnormal cortical development and perisylvian PMG in humans.

2 | SUBJECTS AND METHODS

2.1 | Editorial policies and ethical considerations

Institutional review boards at the Hôpital Universitaire des Enfants Reine Fabiola, the Montreal Neurological Institute, University of Chicago, and Children's Hospital Boston approved this study, and informed consent was obtained for each subject.

2.2 | Patients

We identified a boy with perisylvian PMG in whom duplication 2p13.3-p16.3 was first detected by standard karyotype that was subsequently confirmed and further defined by microarray. We also provide additional data for two previously reported patients with perisylvian PMG in whom large 2p duplications were identified (Dobyns et al., 2008).

2.3 | Genetic analyses

For patient PS-10203, chromosome analysis was performed on 20 metaphases from peripheral lymphocytes using Giemsa banding (GTG banding) according to standard protocols with a resolution level of 450 bands. Fluorescence in situ hybridization (FISH) was performed using a standard protocol with probes RP11-335O22 labeled with ChromaTide® CyTM3 to produce an orange signal, and RP11-304A15 labeled with ChromaTide® Alexa Fluor® 488 to produce a green signal (BlueFISH probe: BlueGnome). Comparative genome hybridization (CGH) was performed using DNA derived from peripheral blood leukocytes on a CytoChip BAC array as described in the manual (BlueGnome) and analyzed using BlueFuse software (BlueGnome). Another aliquot of DNA was digested, amplified, and hybridized to the HumanOmniExpress BeadChip (Illumina, San Diego, CA) to further define the boundaries of the duplicated region. Analysis of the SNP data was performed using Illumina Genome Studios software.

For patients LP99-112 and LR00-173, results of chromosome analysis and BAC arrays were previously described (Dobyns et al., 2008). Subsequently, we performed genome-wide SNP microarrays using the InfiniumII HumanHap610 BeadChip (Illumina San Diego CA), and analyzed the data using PennCNV, to define the boundaries of the duplicated regions according to the methodology described previously (Sajan et al., 2013; K. Wang et al., 2007).

2.4 | Bioinformatics analysis

We first extracted the gene content from the smallest region of overlap of the 2p duplications in the three patients (genome browser: NCBI36/hg18, updated: GRCh38/hg38). We subsequently selected the genes for which there is evidence of expression in developing human brain (Miller et al., 2014). Functional data on these genes were gathered from several databases including OMIM, GeneCards and Gene Ontology (GO), while data on expression in brain was obtained from the Allen Brain Atlas (ABA) and mouse genome informatics (MGI) databases (Finger et al., 2017; Miller et al., 2014; Smith et al., 2014). Hypothetical genes and noncoding genes were excluded. Additional functional data were obtained from the literature and included in the discussion. Protein interaction network analysis was performed with Cytoscape software using Cluego and Cluepedia plug-ins to

TABLE 1 Summary of clinical features of 2p16.1-p16.3 microduplication in three patients

Subject #	PS-10203	LP99-112	LR00-173
Clinical data			
Age at last examination	17 years	16 years	2 weeks (37–38 weeks corrected)
Sex	M	F	M
Fetus	IUGR	IUGR	IUGR; premature, twin
Gestational age	40 weeks	40 weeks	35 3/7 weeks
Measurements at birth			
Weight	2,780 g (4th %ile/−1.77 *SD*)	2,863 g (12th %ile/−1.19 *SD*)	1,532 g (1st %ile/−2.53 *SD*)
Length	48 cm (8th %ile/−1.41 *SD*)	48.3 cm (17th %ile/−0.94 *SD*)	38 cm (0%ile/−3.44 *SD*)
OFC	37 cm (92nd %ile/1.38 *SD*)	34.3 cm (39th %ile/−0.29 *SD*)	32.5 cm (57th %ile/0.17 *SD*)
Weight	$7^{11/12}$ years: 17 kgs (−3.4 *SD*) 12 years: 26 kgs (−2.6 *SD*) 16.5 years: 47.25 kgs (−1.9 *SD*)	9 months: 6.8 kgs (2nd %ile) 2.5 years: 9.3 kgs (−4 *SD*) 16 years: 29.5 kg (−4 *SD*)	
Height	$7^{11/12}$ years: 103.7 cm (−4.3 *SD*) 12 years: 129 cm (−2.7 *SD*) 16.5 years: 153.7 cm (−2.8 *SD*)	9 months: 65 cm (2nd %ile) 2.5 years: 79.6 cm (−4 *SD*) 16 years: 138 cm (−4 *SD*)	
OFC	$7^{11/12}$ years: 54.2 cm (92nd %ile) 12 years: 56 cm (94th %ile)	9 months: 44.5 cm (50th %ile) 2.5 years: 48.5 cm (50th %ile); 5 years 4 months: 49.5 cm (24th % ile) 15 years: 53 cm (14th %ile)	
Facial features	Frontal bossing Hypertelorism Broad nasal bridge Low set ears	Hypertelorism Broad nasal bridge Low set ears Webbing of the neck	Rounded head contour Prominent occiput Mild hypertelorism Low-set and posteriorly-rotated ears Mild corneal clouding Upturned nares Mildly small jaw
Cardiac malformations	Echocardiogram as an infant showed mild pulmonary artery stenosis.	No (unconfirmed heart murmur)	No
Genital malformations	Unilateral cryptorchidism	No	Hypospadias with mid-shaft defect, mild chordee, bilateral undescended testes with R testis palpable but L testis not palpable, mildly small but normally formed scrotum, and bilateral small hydroceles
Feeding	Severe difficulties in neonatal and postnatal period (buccofacial hypotonia and dyspraxia)	Poor appetite	Severe feeding difficulties
Developmental delay	In all areas	Global developmental delay, later able to walk with unsteady gait, limited language	Too young to assess
Motor	Moderate		
Speech	Severe		
Cognitive	Severe		
Epilepsy Seizure type(s)	Possible seizure at 16 months	Yes. Episodes of staring and jerking noted at 15 years. EEG showed generalized slowing of background.	N/A
Behavior	Attention deficit, hyperactivity	Frequent mood swings with agitation and aggression, temper tantrums.	N/A
Sleep	Normal	Alternating periods of too little and excessive sleep	N/A
Eye exam	Left convergent strabismus, normal vision	Strabismus (surgically repaired)	Mild corneal clouding

(Continues)

TABLE 1 (Continued)

Subject #	PS-10203	LP99-112	LR00-173
Ear exam	Unilateral hearing loss (following recurrent otitis)	Normal	N/A
Neurological exam	Neonatal: global hypotonia	N/A	Neonatal: Normal
Age	12 years	16 years	
Cognitive	Moderate ID	Moderate ID	
Speech	Up to three-word sentences	Limited language	
Motor	No longer hypotonic	Unsteady gait	
Brain MRI			
Polymicrogyria	Perisylvian	Perisylvian	Perisylvian
Most severe region	Bilateral fronto-basal, right parieto-occipital	Diffuse, most severe in posterior frontal, perisylvian and parietal regions	Diffuse, all regions affected
Symmetry	R > L	R = L	R = L
Heterotopia	None	None	None
Lateral ventricles	Normal	Normal	Mild dilatation
Midline structures	Normal	Normal	Normal
Cerebellum	Abnormal orientation of sulci over inferior cerebellum	Normal	Normal
White matter	Changes consistent with gliosis anterior to the R lateral ventricle	Normal	Normal
Other	Changes suggesting prior hemorrhages near the R caudate nucleus	None	Colpocephaly, cavum septum vergae
2p duplication	2p13.3-p16.3	2p16.1-p23.1	2p13.1-p24.1
Duplication size			
SNP array [hg38]	chr2:51,428,207–72,007,730	chr2:30,133,795–60,375,757	chr2:21,098,286–64,469,368
The shortest region of overlap [hg38]	51,428,207–60,375,757		
Flanking SNPs	rs13387812 and rs17559295		
Duplicated start and end SNPs		rs11127258 and rs243034	rs534100 and rs962423

Abbreviations: ID, intellectual disability; %ile, centile; IUGR, intrauterine growth restriction; N/A, not available; OFC, occipito-frontal circumference; rs, refSNP; *SD*, standard deviation; SNP, single nucleotide polymorphism.

query GO Molecular Function, GO Biological Process, Kyoto Encyclopedia of Genes and Genomes (KEGG), and Reactome databases (Bindea et al., 2009; Bindea, Galon, & Mlecnik, 2013; Shannon et al., 2003). Pathways were selected that included two or more of the 23 genes in the 2p16.1-p16.3 region with evidence for expression in developing human brain, and had *p*-values <0.05 following Benjamini-Hochberg correction.

3 | RESULTS

The clinical features including neuroimaging findings, as well as results of SNP microarrays are summarized in Table 1 for all three patients.

3.1 | Patient PS-10203

This boy is the third child of healthy non-consanguineous Caucasian parents (Belgian father and Italian mother), and has two healthy sisters. His mother reported diminished fetal movements during the seventh month of her pregnancy. Fetal ultrasound examination revealed intrauterine growth restriction (IUGR) and decreased fetal movements. He was born at 40 weeks gestation by normal spontaneous vaginal delivery. Apgar scores were 8 at 1 min and 10 at 5 min, although placental abruption was noted at delivery. Birth weight was 2,780 g (4th centile), length 48 cm (8th centile), and occipitofrontal circumference (OFC) 37 cm (92nd centile) using the Fenton scales. His neonatal exam demonstrated global hypotonia with greater left than right side involvement, and a poor suck that led to weight loss. His course was complicated by pyloric stenosis treated by pyloromyotomy at 2 weeks. Despite this, feeding difficulties continued and were attributed to hypotonia, weak suck, and poorly coordinated swallowing. An event of unclear significance, possibly a seizure, was observed at 16 months of age. He was treated with phenobarbital for 1 year without any subsequent recognized epilepsy.

His psychomotor development was delayed. He first sat without support at 17 months, walked alone at 40 months, and spoke his first words a few months later. During his first year of life, an

echocardiogram showed mild pulmonary artery stenosis. Subsequent health problems included short stature, recurrent bronchitis, laryngotracheomalacia, and chronic otitis media in the left ear. At 7.5 years, evaluation of growth hormone function with a dynamic glucagon test was normal with a peak level of 22.5 ng/ml (normal >10 ng/ml) and low IGF-1 level. At $7^{11/12}$ years, his height was 103.7 cm (4.3 *SD* below the mean), weight 17 kg (3.4 *SD* below the mean) using UK Cole curves, and OFC 54.2 cm (92nd centile using the Nellhaus curves). His facial appearance was dysmorphic with relative macrocephaly, dolichocephaly, frontal bossing, hypertelorism, broad nasal bridge, thick eyebrows, strabismus, thick upper lip, and low-set, posteriorly rotated and mildly malformed ears (Figure 1a,b). Developmentally, he was able to correctly pronounce 15 words and accurately point to pictures. He had both attention and fine motor deficits. Treatment with human growth hormone was started as no catch-up growth was observed. Bone age was 5 years at a chronological age of 8 years 2 months. At 12 years, his weight was 26 kg (2.6 *SD* below the mean), height 129 cm (2.7 *SD* below the mean), and OFC 56 cm (94th centile). His oromotor control and feeding had improved, and his receptive language was better than his expressive language. He was able to use about 120 words and formulate a few 3–4 word sentences. He was able to use both hands for all daily activities, with a right-hand preference, but with poor fine motor coordination. His strength and tone were normal. His gait was still slightly unstable, with a mildly widened base. He was able to ride a scooter. Compliance to growth hormone treatment was good, and treatment was stopped at 16.5 years when his height was 153.7 cm (2.8 *SD* below the mean), weight 47.25 kg (1.9 *SD* below the mean), puberty stage A2P4G3–4, and bone age 17–18 years. At 17 years, endocrine testing showed normal thyroid function, increased FSH reflecting a gonadal insufficiency mostly regarding spermatogenesis, adult level of testosterone, and normal IGF-1. A glucagon dynamic test showed an acceptable level of growth hormone. Limited metabolic testing was negative.

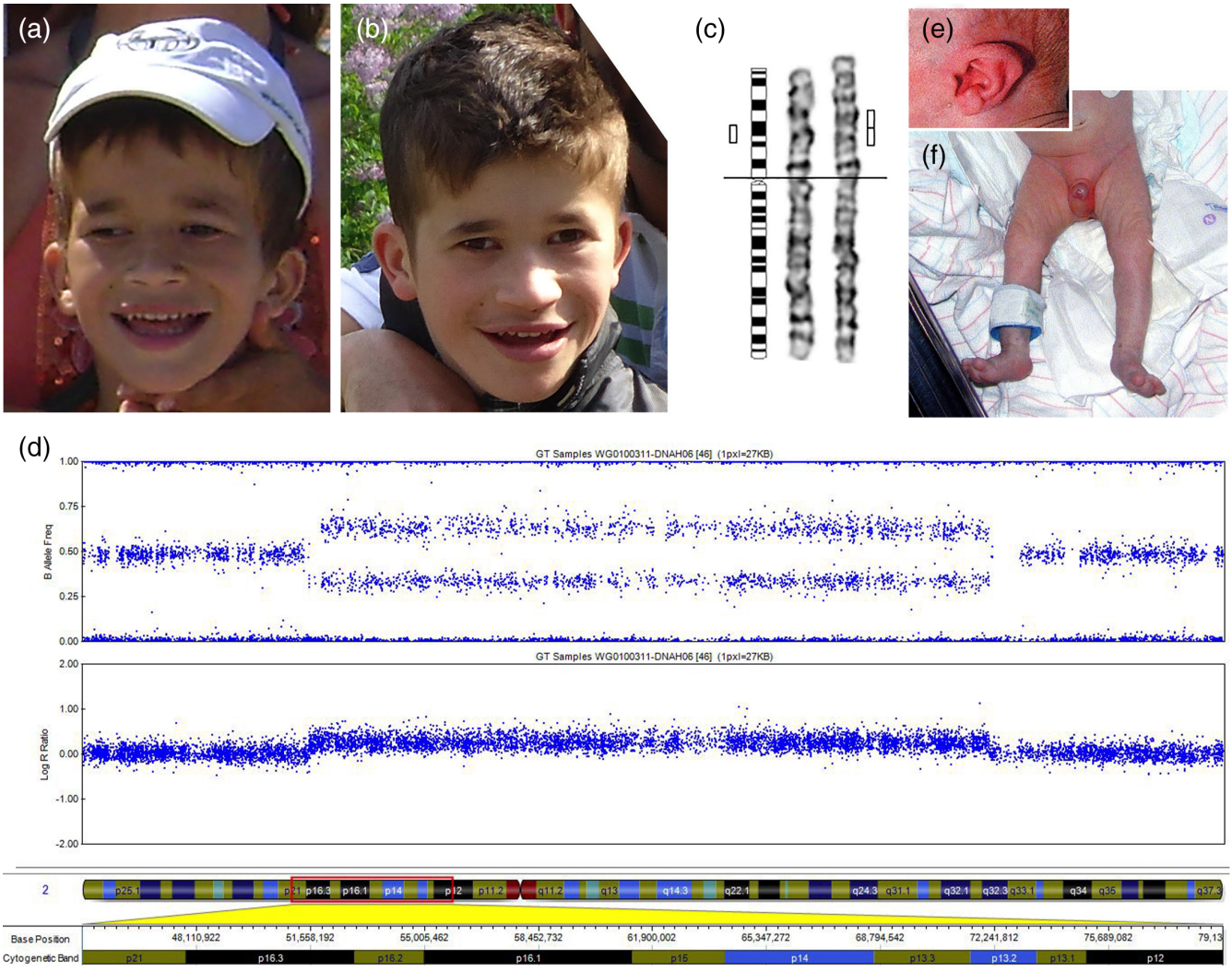

FIGURE 1 Photographs of patient PS10203 at 12 years (a) and 16 years (b) showing thick eyebrows, hypertelorism, broad nasal bridge, thick upper lip, and low-set mildly dysplastic ears. Patient PS10203: Ideogram of chromosome 2p (c) and SNP array (d) showing the 2p duplication. Photographs of patient LR00-173 showing low-set and posteriorly rotated ear (e), hypospadias with mid-shaft defect, mild chordee, mildly small but normally formed scrotum, and bilateral small hydroceles (f)

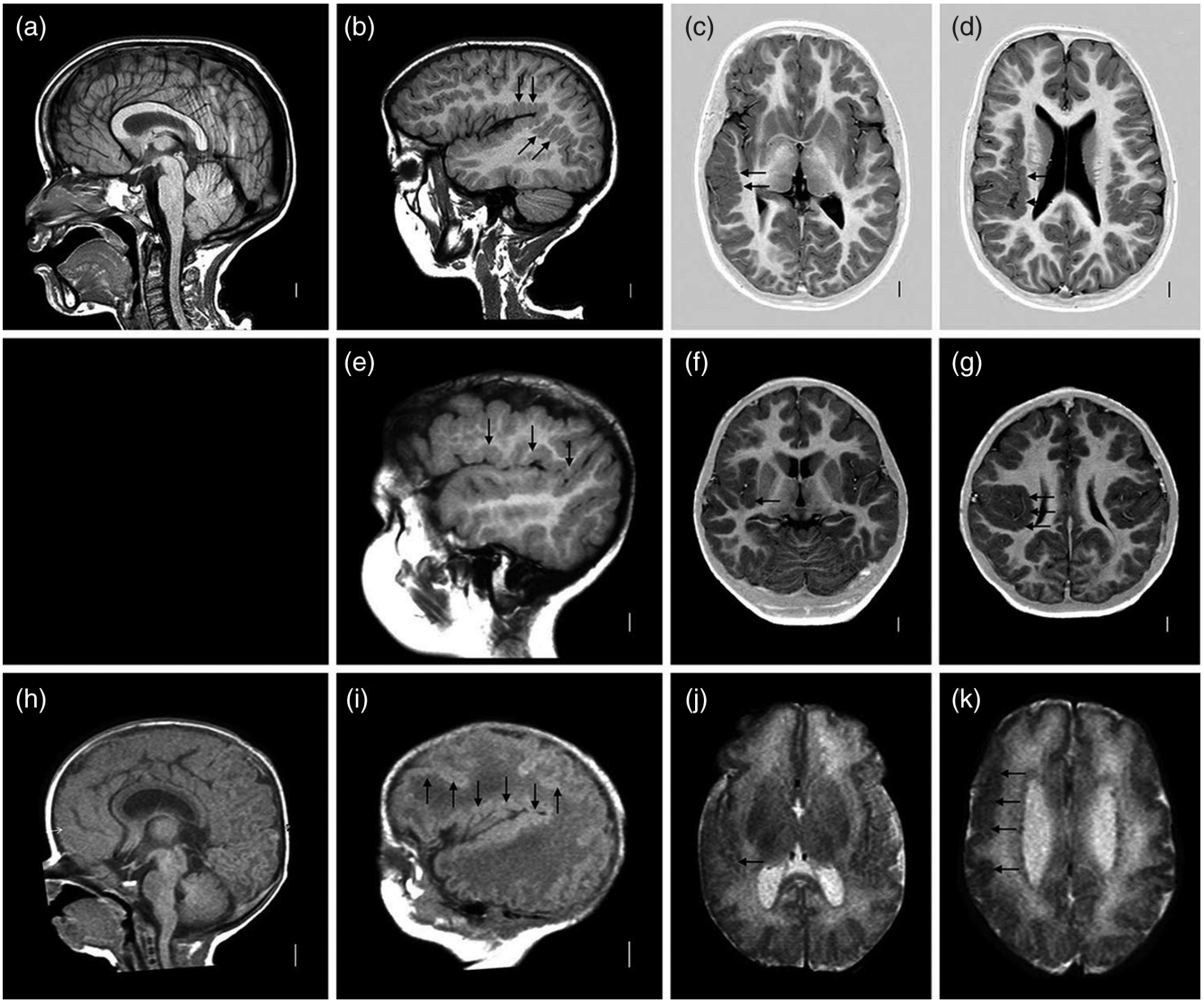

FIGURE 2 Brain magnetic resonance images in subjects PS-10203 (a–d), LP99-112 (e–g) and LR00-173 (h–k) with intrachromosomal 2p duplication. Midline sagittal images in two children (a, h) revealed mildly prominent foreheads with normal midline brain structures. Parasagittal images through the Sylvian fissure (b, e, i) and axial images at the level of the basal ganglia (c, f, j) or high lateral ventricles (d, g, k) show polymicrogyria (black arrows) in the perisylvian regions with extension posteriorly in patient PS-10203 (lower black arrows in b) or anteriorly in patients LP99-112 (e–g) and LR00-173 (i–k)

Brain magnetic resonance imaging (MRI) (Figure 2a–d) was performed twice, and showed BPP extending from the anterior–inferior frontal regions to the temporal lobes with some extension to the parietal lobes, particularly in the right parieto-occipital region; white matter changes consistent with gliosis anterior to the right lateral ventricle; and signal changes suggestive of prior hemorrhages near the right caudate nucleus. Abnormal orientation of several sulci over the inferior cerebellum was seen, but the vermis had normal morphology.

3.2 | Patient LP99-112

This girl was born to healthy non-consanguineous Caucasian parents. Fetal ultrasound revealed IUGR. She was born at term with birth weight 2,863 g (12th centile), length 48.3 cm (17th centile) and OFC 34.3 cm (39th centile) using the Fenton scales. Her postnatal growth was slow with weight and length down to the second centile by 9 months, and down to 4 *SD* below the mean by 2.5 years of age. At 16 years, her weight was 29.5 kg and height 138 cm (both 4 *SD* below the mean). Her OFC was 53 cm (14th centile) at 15 years, using the Nellhaus curves. Serial examinations demonstrated hypertelorism, broad nasal bridge, and low-set ears, as well as strabismus that was surgically repaired. She also had mild webbing of the neck and bilateral elbow contractures. She was able to walk but with an unsteady gait.

Patient LP99-112 had a history of behavioral problems that worsened during adolescence. These consisted of frequent mood swings with agitation, aggression, and temper tantrums. She had variable sleep problems that alternated between too little and excessive sleep. She had onset of seizures consisting of staring and jerking at 15 years. EEG showed generalized background slowing.

Brain MRI (Figure 2e–g) performed at 11 years of age using turbo spin echo and T1-weighted sequences showed bilateral diffuse PMG most severe in the posterior frontal, perisylvian and parietal regions and somewhat less severe in the temporal and inferomesial occipital regions. The cortex was thick measuring 5–7 mm. The lateral ventricles, corpus callosum, brainstem, and cerebellum were normal.

3.3 | Patient LR00-173

This boy was the first child of healthy non-consanguineous Caucasian parents. The pregnancy was conceived by artificial insemination, and complicated by chronic maternal hypertension. Prenatal ultrasound exams detected asymmetric IUGR and possible hypospadias, but prenatal chromosome analysis was declined. Labor was induced at $35^{3/7}$ weeks gestation because of persistent nonreactive stress tests. Fetal heart rate decelerations with onset of contractions led to C-section delivery. His Apgar scores were 7 at 1 min and 9 at 5 min. His birth weight was 1,532 g (first centile, 2.5 *SD* below the mean), length 38 cm (0th centile, 3.44 *SD* below the mean), and OFC 32.5 cm (57th centile) using the Fenton scales. Newborn exam demonstrated several dysmorphic features including rounded head contour, prominent occiput, mild hypertelorism, bilateral low-set and posteriorly rotated ears (Figure 1e), upturned nares, and mildly small jaw. Mild corneal clouding was noted as well. He also had hypospadias with mid-shaft defect, mild chordee, bilateral undescended testes with the right testis palpable and the left testis not palpable, mildly small but normally formed scrotum, and bilateral small hydroceles (Figure 1f). Renal ultrasound was normal. No follow-up was available beyond the newborn period.

Brain MRI (Figure 2h–k) using spin echo and T2-weighted sequences showed symmetric perisylvian PMG extending to most of the brain and associated with mild dilatation of the lateral ventricles, colpocephaly, and cavum septum vergae.

3.4 | Genetic findings

For patient PS-10203, cytogenetic testing revealed an abnormal karyotype with intrachromosomal 2p duplication: 46,XY,dup(2)(p13.3p16.3) (Figure 1c). Parental karyotypes were normal. FISH performed with probes located on both sides of the duplicated region excluded any parental cryptic inversion. Whole genome BAC array showed a minimal duplication size of 19.24 Mb from RP11-389K20 to RP11-467P9 and a maximal duplication size of 21.69 Mb from RP11-5M9 to RP11-343N14 (arr[hg38] 2p16.3-p13.3(50480102×2,51965051–71204542×3,72166713×2).

For patients LP99-112 and LR00-173, cytogenetic analyses had revealed a 2p duplication, as previously reported (Dobyns et al., 2008). The standard karyotype of LP99-112 showed a de novo 46,XX,dup(2)(p16.1p23.1), and in LR00-173 a de novo 46,XY,dup(2)(p13p23).

High-resolution SNP chromosome microarrays in the three patients defined large 20.6, 30.2, and 43.4 Mb duplications, respectively (Table 1) (Figure 1d, Figure S1). The shortest region of overlap consists of an 8.9 Mb duplicated region in 2p16.3p16.1: chr2:51,428,207–60,375,757 [hg38] (Table 1, Figure 3).

3.5 | Bioinformatics analysis

The shared duplicated region contains 33 genes, to which we added *BCL11A* as it was duplicated in two of three patients and either duplicated or just outside the shared duplicated region in LP99-112. Of these 34 genes, 23 had evidence of expression in the human fetal brain based on data from the Allen Institute developmental transcriptome and BrainSpan databases (Miller et al., 2014). Listed from the highest to the lowest expression in RPKM (reads per kilobase per million), these genes include: *RTN4* (122), *MIR4426* (100), *SPTBN1* (53), *RPS27A* (50), *BCL11A* (35), *PPP4R3B* (previously *SMEK2*)(16), *CCDC88A* (previously *GRDN*)(15.5), *CFAP36* (*CCDC104*) (14), *ERLEC1* (14), *FANCL* (10), *CCDC85A* (6.5), *PSME4* (6.0), *ASB3* (4.5), *MTIF2* (3.5), *ACYP2* (3.4), *VRK2* (2.9), *GPR75* (2.7), *PNPT1* (2.0), *EFEMP1* (1.4), *CHAC2* (1.2), *CLHC1* (*C2orf63*) (1.1), *EML6* (0.6), *C2orf73* (0.1) (Table 2).

Functional network analysis with Cytoscape revealed that several developmentally relevant gene clusters are prominently overrepresented in the 2p overlap region described above (Figure S2, Tables S1 and S2). After Benjamini-Hochberg correction, the most significant cluster was comprised by RPS27A and PSME4, which play roles in cell cycle arrest. Other functional clusters are formed by RTN4, SPTBN1, RPS27A, BCL11A, CCDC88A, and PSME4, which regulate axon growth and guidance. Clusters contributing to WNT (RPS27A, PSME4), interleukin-2 (SPTBN1), insulin (SPTBN1, RPS27A, PSME4), and epidermal growth factor (SPTBN1, RPS27A, PSME4, and EFEMP1) signaling were also found. Additionally, we identified significant enrichment of genes regulating RNA translation and degradation, and posttranslational modification of proteins by phosphorylation, conjugation, and ubiquitination. These results indicate that the etiology of polymicrogyria in our three patients may result from misregulation of morphogen, cytokine, hormonal and growth factor signaling; abnormalities of cell cycle progression and morphogenesis; or neuronal migration, as at least three genes function in neuronal migration (EML6, PPP4R3B, and RTN4).

4 | DISCUSSION

Partial trisomy of the short arm of chromosome 2 most often results from the unbalanced product of various reciprocal translocations, and in a minority of patients from a de novo pure 2p proximal or distal intrachromosomal duplication (Aviram-Goldring et al., 2000). The clinical phenotype of patients with large 2p duplications is heterogeneous, but includes pre- and postnatal growth deficiency, psychomotor retardation and dysmorphism.

The phenotype resulting from pure intrachromosomal 2p duplication has been delineated in only a few individuals (Dobyns et al., 2008; Fryns, Kleczkowska, Kenis, Decock, & Van den Berghe, 1989; Megarbane et al., 1997; Yunis, González, Zuñiga, Torres de Caballero, & Mondragon, 1979). From these data, this 2p duplication syndrome is characterized by normal head size, intellectual disability, and facial dysmorphism consisting of hypertelorism, broad nasal bridge

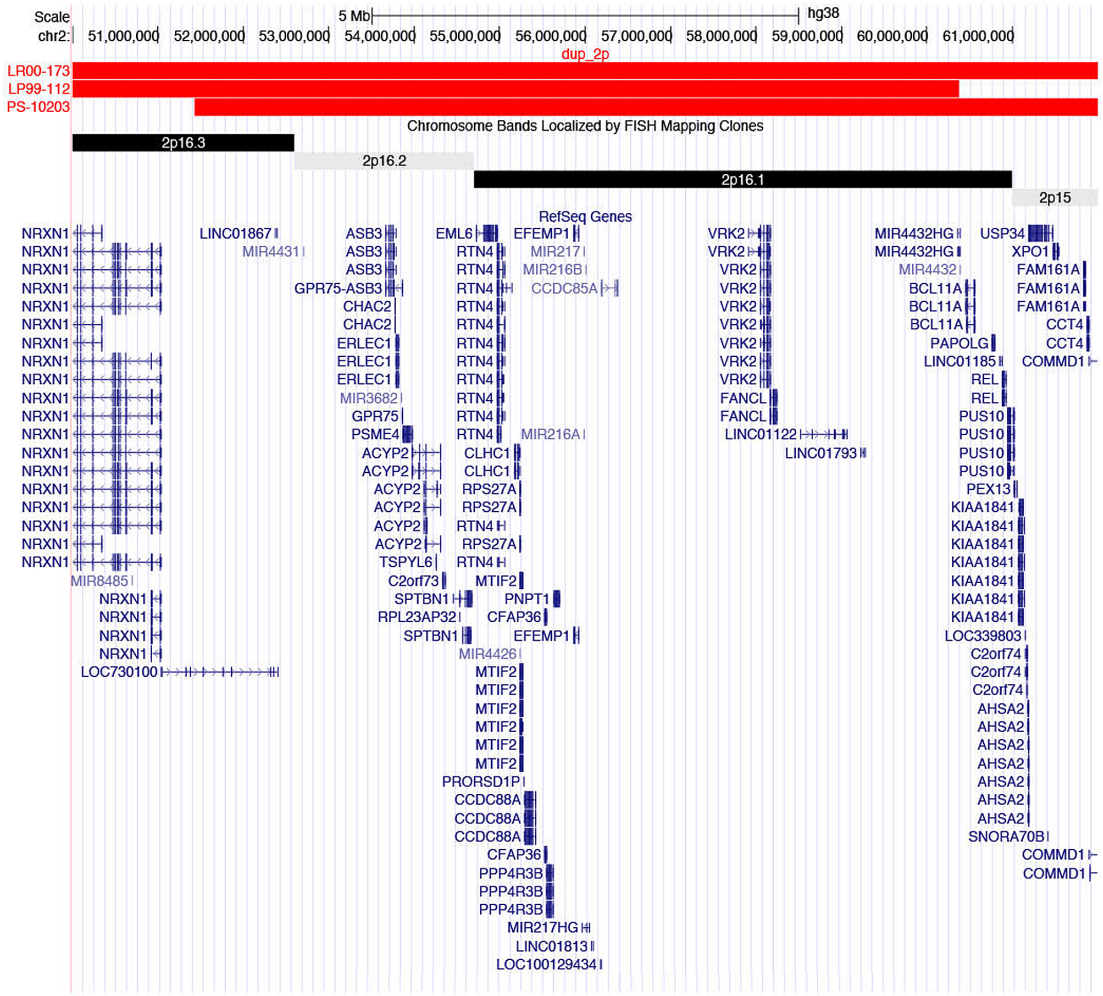

FIGURE 3 An overlapping region of 2p duplication in the three patients represents the shared locus [GRCh38/hg38] [Color figure can be viewed at wileyonlinelibrary.com]

and low-set, malformed ears, with intrauterine and/or postnatal growth deficiency and genital abnormalities such as hypospadias and cryptorchidism. PMG has also been described in our two previously reported patients (LP99-112 and LR00-173) with a 2p duplication (Dobyns et al., 2008). Other reports of patients with a 2p duplication are older and/or not focused on brain malformations or did not include any brain imaging data, so that the presence and type of PMG in these patients is unknown (Aviram-Goldring et al., 2000; Fryns, Kleczkowska, Kenis, Decock, & Van den Berghe, 1989; Megarbane et al., 1997; Yunis et al., 1979). For a number of patients with 2p duplications listed in the DECIPHER database (Firth et al., 2009), there is no brain MRI reported. This database includes data on three individuals with small duplications involving the middle part of our locus, each of which was inherited from a normal parent. No phenotypic data were provided. Furthermore, no benign copy number variants of this region have been reported in the Database of Genomic Variants (http://dgv.tcag.ca/dgv/app/home).

Our three patients have symmetric perisylvian PMG, which is more widespread in the two patients with larger 2p duplications. All three share common phenotypic features including IUGR with head size in the normal range, intellectual disability, and facial dysmorphism consisting of hypertelorism, broad nasal bridge and low-set ears as well as short stature. Considering the common phenotypic features of these three patients, we used SNP array analysis to allow accurate identification of the 2p duplication overlap region and fine mapped a shared locus on chr2:51,428,207–60,375,757 [GRCh38/hg38].

Of the 33 (34 including *BCL11A*) genes extracted for analysis within this shared locus, 22 (23 genes including *BCL11A*) had evidence for expression in human prenatal brain (Table 2). Among these, a number of genes have known functions in brain development. Among genes identified in the shared locus, several are involved in cytoskeletal dynamics: (a) *EML6* (*Homo sapiens* echinoderm microtubule associated protein like 6) codes for a microtubule-associated protein, and *CCDC88A* binds with microtubules (b) *CLHC1* codes for a protein interacting with the microtubule-associated protein MAP1LC3, and (c) *ASB3* is involved in the transport of tubulin. Interestingly, the disruption of *EML6* paralog *EML1* leads to ectopic neuronal progenitors. Biallelic mutations in *EML1* cause a complex brain malformation consisting of megalencephaly, unusual subcortical ribbon heterotopia, polymicrogyria and corpus callosum agenesis (Kielar et al., 2014). The

TABLE 2 Genes within shared 2p duplication locus with evidence for prenatal brain expression

Gene	Entrez gene/HGNC ID	Function	Expression in prenatal brain	
			Mice (*Mus musculus*) (MGI–ABA)	Human (ABA)[a]
RTN4	57142/14085	Protein binding, poly(A) RNA binding. Developmental neurite growth regulatory factor. Regulates the radial migration of cortical neurons.	Radial precursor/glial cells and tangentially migrating as well as postmigratory cortical neurons ND in ABA	122
MIR4426	100616345/41848	No specific data.	ND	100
SPTBN1	6711/11275	Actin binding, protein binding, calmodulin binding, phospholipid binding. Membrane assembly, Golgi to plasma membrane transport. Structural constituent of cytoskeleton. Actin filament capping. Axon guidance.	Cerebral cortex. ND in ABA	53
RPS27A	6233/10417	Structural constituent of ribosome. Protein binding, poly(A) RNA binding, metal ion binding.	ND	50
BCL11A ‡	53335/13221	Zinc-finger protein. Nucleic acid binding, metal ion binding. Transcription corepressor activity, protein homodimerization activity.	ND	35
PPP4R3B (SMEK2)	57223/29267	Protein binding. May regulate the activity of PPP4C at centrosomal microtubule organizing centers.	ND	16
CCDC88A (GRDN)	55704/25523	Protein binding, phosphatidylinositol binding. Actin binding, microtubule binding. Protein homodimerization activity, regulation of actin cytoskeleton organization, cell migration, lamellipodium assembly.	ND	15.5
CFAP36 (CCDC104)	112942/30540	Cilia- and flagella-associated protein. May act as an effector for ARL3 which is a small GTP-binding protein required for normal cytokinesis and cilia signaling.	ND	14
ERLEC1	27248/25222	Protein binding. ER-associated ubiquitin-dependent protein catabolic process.	ND	14
FANCL	55120/20748	Protein binding, zinc ion binding. Ubiquitin-protein ligase activity, ligase activity, ubiquitin protein ligase binding, DNA repair.	Telencephalon ventricular layer, olfactory cortex ventricular layer ND	10
CCDC85A	114800/29400	ND	Diencephalon lateral wall mantle layer, telencephalon mantle layer, medulla oblongata basal plate mantle layer, pons mantle layer, midbrain mantle layer ND in ABA	6.5
PSME4	23198/20635	Protein binding. Peptidase activator activity, histone acetyl-lysine binding.	ND	6.0
ASB3	51130/16013	Protein binding. Intracellular signal transduction. Protein ubiquitination. Involved in the transport of tubulin.	Cerebral cortex and asb3 cerebral cortex ventricular layer. ND in ABA	4.5
MTIF2	4528/7441	Mitochondrial translation initiation factor activity, GTPase activity, GTP binding, nucleic acid binding, ribosomal small subunit binding. One of the essential components for the initiation of protein synthesis.	ND	3.5
ACYP2	98/180	Acylphosphatase activity. Its physiological role is not yet clear.	ND	3.4

(Continues)

TABLE 2 (Continued)

Gene	Entrez gene/HGNC ID	Function	Expression in prenatal brain	
			Mice (*Mus musculus*) (MGI–ABA)	Human (ABA)[a]
VRK2	7444/12719	Protein binding, ATP binding. Protein serine/threonine kinase activity that regulates several signal transduction pathways.	Cerebral cortex and in cerebral cortex marginal layer ND in ABA	2.9
GPR75	10936/4526	Integral component of plasma membrane. G protein-coupled receptor. May play a role in neuron survival.	ND	2.7
PNPT1	87178/23166	Protein binding, poly(U) RNA binding. Implicated in numerous RNA metabolic processes, including import of RNA into the mitochondria. Plays a role in mitochondrial morphogenesis and respiration.	ND	2.0
EFEMP1	2202/3218	Epidermal growth factor-activated receptor activity which activates down signaling pathways. May play a role in cell adhesion and migration.		1.4
CHAC2	494143/32363	The encoded protein catalyzes the conversion of glutathione to 5-oxoproline and cysteinylglycine. It is thought that this gene is upregulated in response to endoplasmic reticulum stress and that the glutathione depletion enhances apoptosis.	ND	1.2
CLHC1 (C2orf63)	130162/26453	Codes for a protein interacting with the microtubule-associated protein MAP1LC3.	ND	1.1
EML6	400954/35412	May modify the assembly dynamics of microtubules.	ND	0.6
C2orf73	129852/26861	Uncharacterized.	ND	0.1

Note: List of genes within 2p duplication locus with no evidence for prenatal brain expression, according to MGI-ABA, with HGNC ID in brackets: MIR4431 (41738), MIR3682 (38916), TSPYL6 (14521), RPL23AP32 (25345), PRORSD1P (34379), MIR217HG (50537), MIR217 (31594), MIR216A (31593)[b], MIR216B (33668)[b], MIR4432HG (partly in [partly out of] the locus) (5205), MIR4432 (just barely out of the locus, probably duplicated as well) (41649).
Abbreviations: ABA, Allen Brain Atlas; Entrez Gene (https://www.ncbi.nlm.nih.gov/gene); ER, endoplasmic reticulum; GO, gene ontology; HGNC, HUGO gene nomenclature committee (https://www.genenames.org/); MGI, mouse genome informatics; ND, no data available; RPKM, reads per kilobase per million.
[a]Expression level in RPKM (average of all prenatal weeks).
[b]These genes were found to be highly expressed during mouse central nervous system development (Dogini, Ribeiro, Rocha, Pereira, & Lopes-Cendes, 2008).

EML proteins contain a domain potentially contributing to tubulin binding (Eichenmüller, Everley, Palange, Lepley, & Suprenant, 2002). The *CCDC88A* gene encodes a key modulator of the AKT–mTOR pathway (Anai et al., 2005). *CCDC88A* is expressed by neuroblasts in development (Enomoto et al., 2009; Y. Wang et al., 2011) and in adult hippocampal progenitor pools (Kim et al., 2009), where it contributes to the establishment of cell polarity (Ohara et al., 2012), at least in part through Par-3 (Ohara et al., 2012) and AKT (Kim et al., 2009). *CCDC88A* also plays essential roles in cytoskeleton remodeling during cell migration (Ohara et al., 2012; Y. Wang et al., 2011).

The *SPTBN1* gene encodes the spectrin protein interconnecting short actin filaments (Goellner & Aberle, 2012). As a major cytoskeletal protein, spectrin has multiple physiological functions, and plays important roles throughout nervous system development and maintenance. Spectrin regulates cell morphology and function, acting at the nuclear envelope and the plasma membrane of axonal and dendritic processes, regulating the formation of paranodes, axon initial segments, and synapses (Zhang, Susuki, Zollinger, Dupree, & Rasband, 2013). Spectrins also interact directly with various cell adhesion molecules, including L1CAM and the neural cell adhesion molecule (NCAM) contributing to neurite outgrowth and synapse function (Machnicka et al., 2014).

Another gene duplicated in our PMG patients is Reticulon 4 (*RTN4*; also known as *NOGO*), known to play important roles in brain morphogenesis. Nogo-A interacts with α-tubulin and the actin cytoskeleton (Oertle & Schwab, 2003) regulating actomyosin contraction, destabilization of microtubules, integrin activation, and gene expression (Schmandke, Schmandke, & Schwab, 2014). Recent studies have uncovered multiple roles of Nogo-A in the orchestration of CNS development at various stages, ranging from cell migration, axon guidance and fasciculation, dendritic branching, and CNS plasticity to oligodendrocyte differentiation and myelination (Schmandke, Schmandke, & Schwab, 2014). In vitro and in vivo studies of the developing mouse cortex have shown that Nogo-A is expressed in

radial glia, radially and tangentially migrating neuronal precursors as well as in postmigratory neurons. Numerous studies further indicate that Nogo-A influences radially migrating principal cortical neurons and tangentially migrating cortical interneurons, as well as neurite formation and guidance (Mingorance-Le Meur, Zheng, Soriano, & Del Río, 2007). Other studies indicate that Nogo signaling impinges on mammalian target of rapamycin (mTOR) and signal transducer and activator of transcription 3 (STAT3) (Gao et al., 2010; B. Wang et al., 2008), and that overexpression of Nogo-A may have neurotoxic effects (Zhong et al., 2016).

EFEMP1 encoded protein, also known as fibulin-3, plays roles in cell adhesion and migration, it may regulate glial cell migration and differentiation as well as the ability of glial cells to support neuronal neurite outgrowth. Studies of loss and gain of function of *EFEMP1* in pancreatic ductal adenocarcinoma showed that EFEMP1 downstream signaling activates Akt- and mitogen-activated protein kinase (MAPK)-signal transduction (Camaj et al., 2009), and the PI3K/mTOR pathway (Diersch et al., 2012). Involvement of this pathway during embryonic development could be possible, although it needs confirmation. The *ASB3* encoded protein contains ankyrin repeat sequence and SOCS box domain. Ankyrins have many known binding partners, including molecules involved in cell adhesion such as L1CAMs, CD44, E-cadherin, ion channels, and in cellular transport such as tubulin and clathrin. GPR75 is a member of the G protein-coupled receptor family. GPR75 together with RANTES is involved in a downstream signaling pathway involving the PI3, Akt, and MAP kinases (Ignatov, Robert, Gregory-Evans, & Schaller, 2006). *VRK2* encoded protein is a serine/threonine kinase that regulates several signal transduction pathways. Overexpression of VRK2A was shown to have a modulatory effect on the signal mediated by MAPK (Fernandez et al., 2012).

BCL11A encoded protein is highly expressed during development of the mouse telencephalon and involved in molecular networks during mouse cerebral corticogenesis (Leid et al., 2004). The gene was duplicated in two of our three patients, and possibly duplicated or disrupted in patient LP99-112, as the centromeric breakpoint was located very close to the gene.

Mutations in some of these genes are known to be associated with neurodevelopmental disorders. *CCDC88A* mutations cause progressive encephalopathy with oedema, hypsarrhythmia and optic atrophy (PEHO)-like syndrome (Nahorski et al., 2016), *VRK2* is associated with autism and neuroectodermal developmental disorders in the 2p15-p16.1 deletion syndrome (Chabchoub, Vermeesch, de Ravel, de Cock, & Fryns, 2008; de Leeuw et al., 2007; Rajcan-Separovic et al., 2007), *BCL11A* haploinsufficiency can be associated with intellectual developmental disorders and cerebellar hypoplasia (Shimbo et al., 2017) as well as hypoplasia of the corpus callosum and a simplified cortical gyral pattern (Balci, Sawyer, Davila, Humphreys, & Dyment, 2015) or a severe speech sound disorder (Peter, Matsushita, Oda, & Raskind, 2014). In the 2p16.1p15 microduplication, *BCL11A* and *VRK2* duplications are thought to be implicated in the observed intellectual deficiency, but no information is provided regarding a possible associated malformation of cortical development (Chen et al., 2018; Mimouni-Bloch, Yeshaya, Kahana, Maya, & Basel-Vanagaite, 2015).

In addition, several microRNAs (miRNAs) are included in the PMG 2p shared locus. miRNAs regulate posttranscriptional gene expression in numerous genes. Many are specifically expressed during telencephalon development in the embryonic mouse, suggesting a potential role in regulating gene expression during brain development (Bulfone, 2005). It is currently unknown which effect each of these miRNAs might have on single genes, although it is worth noting that MIR216A and MIR216B are highly expressed during mouse CNS development (Dogini, Ribeiro, Rocha, Pereira, & Lopes-Cendes, 2008) and that MIR4426 is highly expressed in human embryonic brain (Table 2).

Pathways identified in our study play roles in developmental processes of cell cycle progression and axon guidance, indicating that the developmental origin of polymicrogyria is most likely not due only to deficits in one developmental process per se, but rather to abnormalities spanning the genesis of cortical cells to cell morphogenesis and target innervation (Figure S2, Tables S1 and S2). These findings are useful in understanding the clinical etiology of PMG and may also provide insight into the basic biology of mechanisms regulating normal cortical and gyral development.

5 | CONCLUSION

We have defined a critical region for perisylvian PMG on chromosome 2p16.1-p16.3 that encompasses 33–34 genes, of which 22–23 are expressed in cerebral cortex during human prenatal development. Using pathway analysis, we showed that a number of the duplicated genes contribute to important neurodevelopmental events including regulation of cell cycle progression, cell morphogenesis, and axon guidance through morphogen, cytokine, hormonal, and growth factor signaling, as well as neuronal migration. These findings comprise a first step in defining the underlying etiology of perisylvian PMG resulting from duplication at this locus.

LIST OF ABBREVIATIONS

aCGH	array comparative genomic hybridization
ABA	Allen Brain Atlas
BPP	bilateral perisylvian polymicrogyria
CNVs	copy number variants
GO	gene ontology
KEGG	Kyoto encyclopedia of genes and genomes
MGI	mouse genome informatics
MRI	magnetic resonance imaging
PMG	polymicrogyria
SNP	single nucleotide polymorphism.

CONFLICT OF INTEREST

The authors declare no potential conflict of interest.

AUTHORS CONTRIBUTIONS

D.A.: project writing, patient recruitment, extraction of functional data of the genes studied, writing the manuscript. A.P.: SNP assay, co-writing of the manuscript. J.G.: bioinformatic data on protein interaction network, co-writing of the manuscript. B.D.: patient recruitment. N.D.: patient recruitment. B.P.: molecular cytogenetics. J.N.: extraction of bioinformatics data from the Allen Brain Atlas and Mouse Genome Informatics. F.A.: revision of the first draft of the manuscript. E.A.: detailed manuscript and proofs revision. C.W.: SNP data, manuscript revision. WB.D.: patient recruitment, SNP assay, manuscript revision.

ACKNOWLEDGMENTS

We wish to thank the families of these children for sharing their medical information with us. We are grateful to Dr. Anne De Leener, Laboratory of Cytogenetics at Hôpital Erasme, Université Libre de Bruxelles, for the karyotype and FISH analysis in the family of Patient PS-10203. We are grateful to Dr. C. Heinrich and Dr. J. Harvengt, Department of Endocrinology, Hôpital Universitaire des Enfants Reine Fabiola, Université Libre de Bruxelles, for the endocrinological data regarding patient PS-10203.

WEB RESOURCES

Allen Brain Atlas www.brain-map.org/
BrainSpan (Atlas of the Developing Human Brain; http://www.brainspan.org/) database [Miller et al., 2014]
Copy number variation database, http://dgv.tcag.ca/dgv/app/home
DECIPHER v8.0 (Database of Chromosomal Imbalance and Phenotype in Humans Using Ensembl Resources), https://decipher.sanger.ac.uk
Ensembl Genome Browser, http://www.ensembl.org/Homosapiens/Info/Index
GeneCards, http://www.genecards.org/
Gene Ontology Consortium, http://www.geneontology.org/
Mouse Genome Informatics www.informatics.jax.org/
Online Mendelian Inheritance in Man (OMIM), http://www.omim.org/
PubMed, http://www.ncbi.nlm.nih.gov/PubMed/
RefSeq http://www.ncbi.nlm.nih.gov/refseq/
http://www.socialstyrelsen.se/rarediseases/perisylviansyndrome
www.stanford.edu/~rnusse/wntwindow.html
UCSC Web browser, http://genome.ucsc.edu/
Gene Expression Omnibus, http://www.ncbi.nlm.nih.gov/geo/

ORCID

Dina Amrom https://orcid.org/0000-0002-0616-9371
Christopher A. Walsh https://orcid.org/0000-0002-0156-2238
William B. Dobyns https://orcid.org/0000-0002-7681-2844

REFERENCES

Anai, M., Shojima, N., Katagiri, H., Ogihara, T., Sakoda, H., Onishi, Y., … Asano, T. (2005). A novel protein kinase B (PKB)/AKT-binding protein enhances PKB kinase activity and regulates DNA synthesis. *Journal of Biological Chemistry*, *280*(18), 18525–18535. https://doi.org/10.1074/jbc.M500586200

Aviram-Goldring, A., Fritz, B., Bartsch, C., Steuber, E., Daniely, M., Lev, D., … Frydman, M. (2000). Molecular cytogenetic studies in three patients with partial trisomy 2p, including CGH from paraffin-embedded tissue. *American Journal of Medical Genetics*, *91*(1), 74–82. http://ovidsp.ovid.com/ovidweb.cgi?T=JS&PAGE=reference&D=emed8&NEWS=N&AN=30127564

Balci, T. B., Sawyer, S. L., Davila, J., Humphreys, P., & Dyment, D. A. (2015). Brain malformations in a patient with deletion 2p16.1: A refinement of the phenotype to BCL11A. *European Journal of Medical Genetics*, *58*(6–7), 351–354. https://doi.org/10.1016/j.ejmg.2015.04.006

Barkovich, A. J., Guerrini, R., Kuzniecky, R. I., Jackson, G. D., & Dobyns, W. B. (2012). A developmental and genetic classification for malformations of cortical development: Update 2012. *Brain: A Journal of Neurology*, *135*(Pt 5), 1348–1369. https://doi.org/10.1093/brain/aws019

Bindea, G., Galon, J., & Mlecnik, B. (2013). CluePedia Cytoscape plugin: Pathway insights using integrated experimental and in silico data. *Bioinformatics*, *29*(5), 661–663. https://doi.org/10.1093/bioinformatics/btt019

Bindea, G., Mlecnik, B., Hackl, H., Charoentong, P., Tosolini, M., Kirilovsky, A., … Galon, J. (2009). ClueGO: A Cytoscape plug-in to decipher functionally grouped gene ontology and pathway annotation networks. *Bioinformatics*, *25*(8), 1091–1093. https://doi.org/10.1093/bioinformatics/btp101

Bulfone, A. (2005). Telencephalic embryonic subtractive sequences: a unique collection of neurodevelopmental genes. *Journal of Neuroscience*, *25*(33), 7586–7600. https://doi.org/10.1523/JNEUROSCI.0522-05.2005

Camaj, P., Seeliger, H., Ischenko, I., Krebs, S., Blum, H., De Toni, E. N., … Bruns, C. J. (2009). EFEMP1 binds the EGF receptor and activates MAPK and Akt pathways in pancreatic carcinoma cells. *Biological Chemistry*, *390*(12), 1293–1302. https://doi.org/10.1515/BC.2009.140

Chabchoub, E., Vermeesch, J. R., de Ravel, T., de Cock, P., & Fryns, J.-P. (2008). The facial dysmorphy in the newly recognised microdeletion 2p15-p16.1 refined to a 570 kb region in 2p15. *Journal of Medical Genetics*, *45*(3), 189–192. https://doi.org/10.1136/jmg.2007.056176

Chen, C. P., Chern, S. R., Wu, P. S., Chen, S. W., Lai, S. T., Chuang, T. Y., … Wang, W. (2018). Prenatal diagnosis of a 3.2-Mb 2p16.1-p15 duplication associated with familial intellectual disability. *Taiwanese Journal of Obstetrics and Gynecology.*, *57*, 578–582. https://doi.org/10.1016/j.tjog.2018.06.018

de Leeuw, N., Pfundt, R., Koolen, D. A., Neefs, I., Scheltinga, I., Mieloo, H., … Knoers, N. V. A. M. (2007). A newly recognised microdeletion syndrome involving 2p15p16.1: Narrowing down the critical region by adding another patient detected by genome wide tiling path array comparative genomic hybridisation analysis. *Journal of Medical Genetics*, *45*(2), 122–124. https://doi.org/10.1136/jmg.2007.054049

Diersch, S., Wenzel, P., Szameitat, M., Eser, P., Paul, M. C., Seidler, B., … Schneider, G. (2012). Efemp1 and p27Kip1 modulate responsiveness of pancreatic cancer cells towards a dual PI3K/mTOR inhibitor in preclinical models. *Oncotarget*, *4*(2), 277–288. https://doi.org/10.18632/oncotarget.859

Dobyns, W. B., Mirzaa, G., Christian, S. L., Petras, K., Roseberry, J., Clark, G. D., … Shaffer, L. G. (2008). Consistent chromosome abnormalities identify novel polymicrogyria loci in 1p36.3, 2p16.1-p23.1, 4q21.21-q22.1, 6q26-q27, and 21q2. *American Journal of Medical Genetics, Part A*, *146*(13), 1637–1654. https://doi.org/10.1002/ajmg.a.32293

Dogini, D. B., Ribeiro, P. A. O., Rocha, C., Pereira, T. C., & Lopes-Cendes, I. (2008). MicroRNA expression profile in murine central nervous system

development. *Journal of Molecular Neuroscience : MN*, *35*(3), 331–337. https://doi.org/10.1007/s12031-008-9068-4

Eichenmüller, B., Everley, P., Palange, J., Lepley, D., & Suprenant, K. A. (2002). The human EMAP-like protein-70 (ELP70) is a microtubule destabilizer that localizes to the mitotic apparatus. *Journal of Biological Chemistry*, *277*(2), 1301–1309. https://doi.org/10.1074/jbc.M106628200

Enomoto, A., Asai, N., Namba, T., Wang, Y., Kato, T., Tanaka, M., … Takahashi, M. (2009). Roles of disrupted-in-schizophrenia 1-interacting protein girdin in postnatal development of the dentate gyrus. *Neuron*, *63*(6), 774–787. https://doi.org/10.1016/j.neuron.2009.08.015

Fernandez, I. F., Perez-Rivas, L. G., Blanco, S., Castillo-Dominguez, A. A., Lozano, J., & Lazo, P. A. (2012). VRK2 anchors KSR1-MEK1 to endoplasmic reticulum forming a macromolecular complex that compartmentalizes MAPK signaling. *Cellular and Molecular Life Sciences*, *69*(22), 3881–3893. https://doi.org/10.1007/s00018-012-1056-8

Finger, J. H., Smith, C. M., Hayamizu, T. F., McCright, I. J., Xu, J., Law, M., … Ringwald, M. (2017). The mouse gene expression database (GXD): 2017 update. *Nucleic Acids Research*, *45*(D1), D730–D736. https://doi.org/10.1093/nar/gkw1073

Firth, H. V., Richards, S. M., Bevan, A. P., Clayton, S., Corpas, M., Rajan, D., … Carter, N. P. (2009). DECIPHER: Database of chromosomal imbalance and phenotype in humans using Ensembl resources. *American Journal of Human Genetics*, *84*(4), 524–533. https://doi.org/10.1016/j.ajhg.2009.03.010

Fryns, J. P., Kleczkowska, A., Kenis, H., Decock, P., & Van den Berghe, H. (1989). Partial duplication of the short arm of chromosome 2 (dup(2)(p13----p21)) associated with mental retardation and an Aarskog-like phenotype. *Annales de Genetique*, *32*(3), 174–176. http://www.ncbi.nlm.nih.gov/pubmed/2573314

Gao, Y., Wang, B., Xiao, Z., Chen, B., Han, J., Wang, X., … Dai, J. (2010). Nogo-66 regulates nanog expression through Stat3 pathway in murine embryonic stem cells. *Stem Cells and Development*, *19*(1), 53–60. https://doi.org/10.1089/scd.2008.0357

Goellner, B., & Aberle, H. (2012). The synaptic cytoskeleton in development and disease. *Developmental Neurobiology*, *72*(1), 111–125. https://doi.org/10.1002/dneu.20892

Ignatov, A., Robert, J., Gregory-Evans, C., & Schaller, H. C. (2006). RANTES stimulates Ca^{2+} mobilization and inositol trisphosphate (IP_3) formation in cells transfected with G protein-coupled receptor 75. *British Journal of Pharmacology*, *149*(5), 490–497. https://doi.org/10.1038/sj.bjp.0706909

Jansen, A., & Andermann, E. (2005). Genetics of the polymicrogyria syndromes. *Journal of Medical Genetics.*, *42*, 369–378. https://doi.org/10.1136/jmg.2004.023952

Kielar, M., Tuy, F. P. D., Bizzotto, S., Lebrand, C., de Juan Romero, C., Poirier, K., … Francis, F. (2014). Mutations in Eml1 lead to ectopic progenitors and neuronal heterotopia in mouse and human. *Nature Neuroscience*, *17*(7), 923–933. https://doi.org/10.1038/nn.3729

Kim, J. Y., Duan, X., Liu, C. Y., Jang, M. H., Guo, J. U., Pow-anpongkul, N., … Ming, G. l. (2009). DISC1 regulates new neuron development in the adult brain via modulation of AKT-mTOR signaling through KIAA1212. *Neuron*, *63*(6), 761–773. https://doi.org/10.1016/j.neuron.2009.08.008

Leid, M., Ishmael, J. E., Avram, D., Shepherd, D., Fraulob, V., & Dollé, P. (2004). CTIP1 and CTIP2 are differentially expressed during mouse embryogenesis. *Gene Expression Patterns*, *4*(6), 733–739. https://doi.org/10.1016/j.modgep.2004.03.009

Machnicka, B., Czogalla, A., Hryniewicz-Jankowska, A., Bogusławska, D. M., Grochowalska, R., Heger, E., & Sikorski, A. F. (2014). Spectrins: A structural platform for stabilization and activation of membrane channels, receptors and transporters. *Biochimica et Biophysica Acta - Biomembranes*, *1838*(2), 620–634. https://doi.org/10.1016/j.bbamem.2013.05.002

Megarbane, A., Souraty, N., Prieur, M., Theophile, D., Chedid, P., Auge, J., & Vekemans, M. (1997). Interstitial duplication of the short arm of chromosome 2: Report of a new case and review. *Journal of Medical Genetics*, *34*(9), 783–786. http://www.ncbi.nlm.nih.gov/entrez/query.fcgi?cmd=Retrieve&db=PubMed&dopt=Citation&list_uids=9321771

Miller, J. A., Ding, S.-L., Sunkin, S. M., Smith, K. A., Ng, L., Szafer, A., … Lein, E. S. (2014). Transcriptional landscape of the prenatal human brain. *Nature*, *508*(7495), 199–206. https://doi.org/10.1038/nature13185

Mimouni-Bloch, A., Yeshaya, J., Kahana, S., Maya, I., & Basel-Vanagaite, L. (2015). A de-novo interstitial microduplication involving 2p16.1-p15 and mirroring 2p16.1-p15 microdeletion syndrome: Clinical and molecular analysis. *European Journal of Paediatric Neurology.*, *19*, 711–715. https://doi.org/10.1016/j.ejpn.2015.07.013

Mingorance-Le Meur, A., Zheng, B., Soriano, E., & Del Río, J. A. (2007). Involvement of the myelin-associated inhibitor Nogo-a in early cortical development and neuronal maturation. *Cerebral Cortex*, *17*(10), 2375–2386. https://doi.org/10.1093/cercor/bhl146

Nahorski, M. S., Asai, M., Wakeling, E., Parker, A., Asai, N., Canham, N., … Woods, C. G. (2016). CCDC88A mutations cause PEHO-like syndrome in humans and mouse. *Brain*, *139*(4), 1036–1044. https://doi.org/10.1093/brain/aww014

Oertle, T., & Schwab, M. E. (2003). Nogo and its paRTNers. *Trends in Cell Biology.*, *13*, 187–194. https://doi.org/10.1016/S0962-8924(03)00035-7

Ohara, K., Enomoto, A., Kato, T., Hashimoto, T., Isotani-Sakakibara, M., Asai, N., … Takahashi, M. (2012). Involvement of Girdin in the determination of cell polarity during cell migration. *PLoS One*, *7*(5), e36681. https://doi.org/10.1371/journal.pone.0036681

Peter, B., Matsushita, M., Oda, K., & Raskind, W. (2014). De novo microdeletion of BCL11A is associated with severe speech sound disorder. *American Journal of Medical Genetics. Part A*, *164A*(8), 2091–2096. https://doi.org/10.1002/ajmg.a.36599

Rajcan-Separovic, E., Harvard, C., Liu, X., McGillivray, B., Hall, J. G., Qiao, Y., … Lewis, M. E. S. (2007). Clinical and molecular cytogenetic characterisation of a newly recognised microdeletion syndrome involving 2p15-16.1. *Journal of Medical Genetics*, *44*(4), 269–276. https://doi.org/10.1136/jmg.2006.045013

Robin, N. H., Taylor, C. J., McDonald-McGinn, D. M., Zackai, E. H., Bingham, P., Collins, K. J., … Dobyns, W. B. (2006). Polymicrogyria and deletion 22q11.2 syndrome: Window to the etiology of a common cortical malformation. *American Journal of Medical Genetics, Part A*, *140*(22), 2416–2425. https://doi.org/10.1002/ajmg.a.31443

Sajan, S. A., Fernandez, L., Nieh, S. E., Rider, E., Bukshpun, P., Wakahiro, M., … Sherr, E. H. (2013). Both rare and de novo copy number variants are prevalent in agenesis of the corpus callosum but not in cerebellar hypoplasia or polymicrogyria. *PLoS Genetics*, *9*(10), e1003823. https://doi.org/10.1371/journal.pgen.1003823

Schmandke, A., Schmandke, A., & Schwab, M. E. (2014). Nogo-A: Multiple roles in CNS development, maintenance, and disease. *The Neuroscientist*, *20*(4), 372–386. https://doi.org/10.1177/1073858413516800

Shannon, P., Markiel, A., Ozier, O., Baliga, N. S., Wang, J. T., Ramage, D., … Ideker, T. (2003). Cytoscape: A software environment for integrated models of biomolecular interaction networks. *Genome Research*, *13*(11), 2498–2504. https://doi.org/10.1101/gr.1239303

Shimbo, H., Yokoi, T., Aida, N., Mizuno, S., Suzumura, H., Nagai, J., … Kurosawa, K. (2017). Haploinsufficiency of BCL11A associated with cerebellar abnormalities in 2p15p16.1 deletion syndrome. *Molecular Genetics and Genomic Medicine.*, *5*, 429–437. https://doi.org/10.1002/mgg3.289

Smith, C. M., Finger, J. H., Hayamizu, T. F., McCright, I. J., Xu, J., Berghout, J., … Ringwald, M. (2014). The mouse gene expression database (GXD): 2014 update. *Nucleic Acids Research*, *42*(D1), 818–824. https://doi.org/10.1093/nar/gkt954

Stutterd, C. A., & Leventer, R. J. (2014). Polymicrogyria: A common and heterogeneous malformation of cortical development. *American Journal of Medical Genetics, Part C: Seminars in Medical Genetics*, *166*(2), 227–239. https://doi.org/10.1002/ajmg.c.31399

Wang, B., Xiao, Z., Chen, B., Han, J., Gao, Y., Zhang, J., … Dai, J. (2008). Nogo-66 promotes the differentiation of neural progenitors into

astroglial lineage cells through mTOR-STAT3 pathway. *PLoS One*, 3. e1856. https://doi.org/10.1371/journal.pone.0001856

Wang, K., Li, M., Hadley, D., Liu, R., Glessner, J., Grant, S. F. A., … Bucan, M. (2007). PennCNV: An integrated hidden Markov model designed for high-resolution copy number variation detection in whole-genome SNP genotyping data. *Genome Research*, *17*(11), 1665–1674. https://doi.org/10.1101/gr.6861907

Wang, Y., Kaneko, N., Asai, N., Enomoto, A., Isotani-Sakakibara, M., Kato, T., … Takahashi, M. (2011). Girdin is an intrinsic regulator of neuroblast chain migration in the rostral migratory stream of the postnatal brain. *Journal of Neuroscience*, *31*(22), 8109–8122. https://doi.org/10.1523/JNEUROSCI.1130-11.2011

Yunis, E., González, J., Zuñiga, R., Torres de Caballero, O. M., & Mondragon, A. (1979). Direct duplication 2p14 to 2p23. *Human Genetics*, *48*(2), 241–244. http://www.ncbi.nlm.nih.gov/pubmed/457145

Zhang, C., Susuki, K., Zollinger, D. R., Dupree, J. L., & Rasband, M. N. (2013). Membrane domain organization of myelinated axons requires betaII spectrin. *Journal of Cell Biology*, *203*(3), 437–443. https://doi.org/10.1083/jcb.201308116

Zhong, J., Li, X., Wan, L., Chen, Z., Zhong, S., Xiao, S., & Yan, Z. (2016). Knockdown of NogoA prevents MPP+-induced neurotoxicity in PC12 cells via the mTOR/STAT3 signaling pathway. *Molecular Medicine Reports.*, *13*, 1427–1433. https://doi.org/10.3892/mmr.2015.4637

SUPPORTING INFORMATION

Additional supporting information may be found online in the Supporting Information section at the end of this article.

How to cite this article: Amrom D, Poduri A, Goldman JS, et al. Duplication 2p16 is associated with perisylvian polymicrogyria. *Am J Med Genet Part A*. 2019;179A: 2343–2356. https://doi.org/10.1002/ajmg.a.61342